Zircon U-Pb Geochronology Links the End-Triassic Extinction with the Central Atlantic Magmatic Province

Terrence J. Blackburn *et al.*

Science **340**, 941 (2013);
DOI: 10.1126/science.1234204

Zircon U-Pb Geochronology Links the End-Triassic Extinction with the Central Atlantic Magmatic Province

Terrence J. Blackburn,[1*†] Paul E. Olsen,[2] Samuel A. Bowring,[1] Noah M. McLean,[1] Dennis V. Kent,[2,3] John Puffer,[4] Greg McHone,[5] E. Troy Rasbury,[6] Mohammed Et-Touhami[7]

The end-Triassic extinction is characterized by major losses in both terrestrial and marine diversity, setting the stage for dinosaurs to dominate Earth for the next 136 million years. Despite the approximate coincidence between this extinction and flood basalt volcanism, existing geochronologic dates have insufficient resolution to confirm eruptive rates required to induce major climate perturbations. Here, we present new zircon uranium-lead (U-Pb) geochronologic constraints on the age and duration of flood basalt volcanism within the Central Atlantic Magmatic Province. This chronology demonstrates synchroneity between the earliest volcanism and extinction, tests and corroborates the existing astrochronologic time scale, and shows that the release of magma and associated atmospheric flux occurred in four pulses over about 600,000 years, indicating expansive volcanism even as the biologic recovery was under way.

The approximate temporal coincidence between the five major extinction events over the past 542 million years and the eruption of large igneous provinces (LIPs) has led to speculation that environmental perturbations generated by the emplacement of large volumes of magma and associated outgassing over short periods of time triggered each global biologic crisis (*1*). Establishing an exact link between extinctions and LIP eruptions has proved difficult because of the geographic separation between LIP volcanic deposits and stratigraphic sequences preserving evidence of the extinction. In most cases, uncertainties on radioisotopic dates used to correlate between geographically separated study areas exceed the duration of both the extinction interval and LIP volcanism by an order of magnitude. This hinders evaluation of any relationship between magmatism and extinction and precludes accurate estimates of volcanic effusion rates, associated volatile release, and extinction mechanisms.

The end-Triassic extinction (ETE)—marked within early Mesozoic basins of eastern North America by a dramatic turnover in fossil pollen, spores (sporomorphs), and vertebrates (*2*)—is one of the largest Phanerozoic mass extinctions, occurring just before the Triassic-Jurassic boundary (*3*, *4*), and has long been thought to be associated with the eruptions of the Central Atlantic Magmatic Province (CAMP) (*5*, *6*). CAMP is the most aerially extensive LIP on Earth, and with volume estimates between 2–3 × 10^6 km^3, it ranks as one of the most voluminous (*7*) (Fig. 1). Remnants of CAMP are found on four continents and consist primarily of continental thoeliitic basalts emplaced as subaerial flows and intrusive bodies during rifting of the Pangean supercontinent and incipient formation of the Atlantic Ocean basin (Fig. 1). Estimates of the timing and duration of CAMP provided by astrochronology (*8*, *9*) and $^{40}Ar/^{39}Ar$ geochronology (*10*, *11*) differ by an order of magnitude, preventing high-precision tests of the relationship between LIP volcanism and mass extinction. Use of the astrochronologic time-scale, though potentially precise, relies on (i) recognition of the influence of orbital cycles in the rock record and (ii) the ability to predict orbital durations in the deep geologic past, both of which have engendered doubts about the reliability of the technique. The lower precision of $^{40}Ar/^{39}Ar$ dates (fig. S1) prevents estimation of the volume of magma erupted over unit time, a critical factor for evaluating extinction mechanisms such as CO_2-induced global warming (*12*, *13*) ocean acidification (*14*, *15*), or sulfur aerosol–induced "volcanic winters" (*16*).

U-Pb Geochronology of CAMP Flows and Intrusives

Here, we present zircon ($ZrSiO_4$) U-Pb geochronologic data for CAMP magmatism from seven sites in eastern North America and one in Morocco (Fig. 1), integrated with paleobiological, geochemical, and paleomagnetic data derived from sedimentary sequences interbedded with and intruded by the magmatic rocks. These data provide (i) a precise determination of the onset and duration of CAMP magmatism and (ii) a test of the reliability of the astronomical time scale in order to provide a high-precision age model for the CAMP-ETE interval (*8*, *9*). Though U-Pb dating of zircon permits an order of magnitude improvement over previous $^{40}Ar/^{39}Ar$ studies (fig. S1), this preferred mineral for U-Pb dating is uncommon in basaltic rocks. This forced our sample collection to focus on finding isolated coarse-grained segregations within gabbroic intrusions and thick subaerial flows where incompatible element-enriched residual melts resulted in the crystallization of zircon (*17*) (fig. S2). The reported zircon U-Pb dates are ^{238}U-^{206}Pb weighted mean dates with ±2σ analytical uncertainties corrected for initial ^{230}Th disequilibrium (figs. S3 and S4) (*18*).

Stratigraphically constrained basalt flows, such as the North Mountain and Preakness basalts, provide the most straightforward means of directly

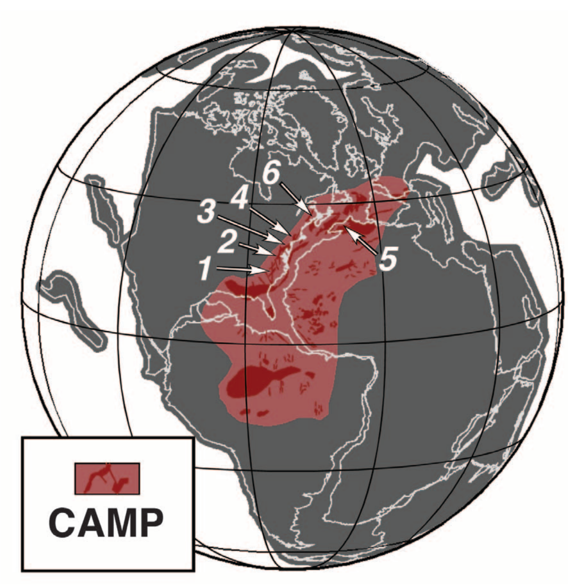

Fig. 1. Location and extent of CAMP magmatism within the Pangean supercontinent. Earliest Jurassic plate configuration showing distribution of the CAMP [based on (*36*, *40*)], including the total areal distribution (pink) and preserved remnants of CAMP (dark red) [based on (*5*)], and the location of the studied basins: 1, Deep River, North Carolina, USA; 2, Culpeper, Virginia, USA; 3, Gettysburg, Pennsylvania, USA; 4, Newark, New Jersey, USA; 5, Argana, Morocco; and 6, Fundy, Nova Scotia, Canada.

[1]Department of Earth, Atmospheric and Planetary Sciences, Massachusetts Institute of Technology, Cambridge, MA 02139, USA. [2]Lamont-Doherty Earth Observatory of Columbia University, Palisades, NY 10964, USA. [3]Department of Earth and Planetary Sciences, Rutgers University, Piscataway, NJ 08554, USA. [4]Department of Earth and Environmental Sciences, Rutgers University, Newark College of Arts and Sciences, Newark, NJ 07102, USA. [5]9 Dexters Lane, Grand Manan, New Brunswick E5G 1A1, Canada. [6]Department of Geosciences, Stony Brook University, Stony Brook, NY 11794, USA. [7]Département des Sciences de la Terre, Université Mohammed Premier Oujda, 60000 Oujda, Morocco.

*Present address: Department of Terrestrial Magnetism, Carnegie Institution for Science, Washington, DC 20015, USA.
†Corresponding author. E-mail: tblackburn@ciw.edu

dating the Triassic and Early Jurassic stratigraphy (Fig. 2). However, coarse-grained zircon-bearing flows in the CAMP are relatively rare. Therefore, we also have dated sills that are either physically connected to flows as feeders or can be geochemically linked with stratigraphically constrained flows (*18*, *19*). In both North American and Moroccan basins, stratigraphic superposition of basalt flows combined with trace element geochemistry provides a relative time scale for the geochemical evolution of CAMP basalts (*11*, *20*–*25*) (Fig. 3A). This same geochemical trend is also observed in the dated stratigraphically unconstrained units (Fig. 3A). The shared geochemical evolution in CAMP magmas permits correlation between units that share a common trace element signature, allowing the U-Pb date for a stratigraphically unconstrained intrusion to effectively date the horizon of a geochemically similar and stratigraphically constrained basalt flow. This composite geochronologically dated stratigraphic section is used to test the astrochronologic time scale for the Newark basin.

Testing the Astrochronologic Time Scale for the Late Triassic

The quasiperiodic variations in Earth's orbit, axial direction, and tilt known as Milankovitch cycles result in corresponding variations in the amount and distribution of sunlight reaching Earth. The resulting forcing on climate and/or ocean circulation can influence the characteristics of sediments deposited within a basin, which may ultimately be preserved within the rock record as cyclical variations in rock lithology, chemistry, or isotopic composition (*26*). CAMP lava flows within the Newark basin of eastern North America (Fig. 2) are interbedded with strikingly cyclical lacustrine strata that have long been hypothesized to be paced by orbital forcing (*27*). Astrochronologic models for these sequences have been used to estimate the time represented by the sedimentary rocks between CAMP flows, placing high-precision [±20 thousand years (ky)] estimates on the total duration of the CAMP at between 580 and 610 ky (*9*, *28*). This proposed "floating" astronomical time scale (ATS) has been met with scrutiny because of the possibility that Earth experienced a different orbital forcing deep in geologic time due to differences in the state of the Earth-Moon system and solar systems dynamics. Further skepticism has focused on whether orbitally forced climatic effects are both accurately recorded and recognized in the geological record. The most straightforward test of the reliability of the ATS is to compare the time durations between basalt flows estimated by orbitally tuning the sedimentary rocks with differences between the zircon U-Pb dates of the flows.

The Orange Mountain Basalt flows are the oldest CAMP lavas in the Newark basin. Although authigenic zircons were not recovered from the Orange Mountain Basalt samples, the flow sequence is partly intruded and fed by an extension of the geochemically identical Palisade sill [201.520 ± 0.034 million years ago (Ma)] (*19*). Based on the ATS for the Newark basin, the overlying flows of the Preakness Basalt should be 250 ± 20 ky younger than the Orange Mountain Basalt (and Palisade sill) (*9*). The U-Pb date of the Preakness Basalt (201.274 ± 0.032 Ma) results in a difference of 246 ± 47 ky, consistent with the astrochronological estimate. A second interval within the Newark ATS, that again uses the Preakness basalt, can be tested by correlating the Butner diabase from the Deep River Basin (200.916 ± 0.064 Ma) to the stratigraphically highest and geochemically similar Hook Mountain Basalt (Fig. 3A). The ATS estimate for the time interval between the base of the Preakness and the base of the Hook mountain basalts is 350 ± 20 ky, a duration consistent with the difference between U-Pb dates for the Preakness Basalt and the Butner sheet of 358 ± 72 ky.

A more complete test of the ATS is provided by comparing the astronomical time scale to each of the CAMP flows and intrusions dated here. Using the relative stratigraphy of preserved CAMP flows and the geochemical correlations (Fig. 3A), each stratigraphically unconstrained CAMP intrusive can be correlated to the astronomically tuned Newark Basin. By correlating to the

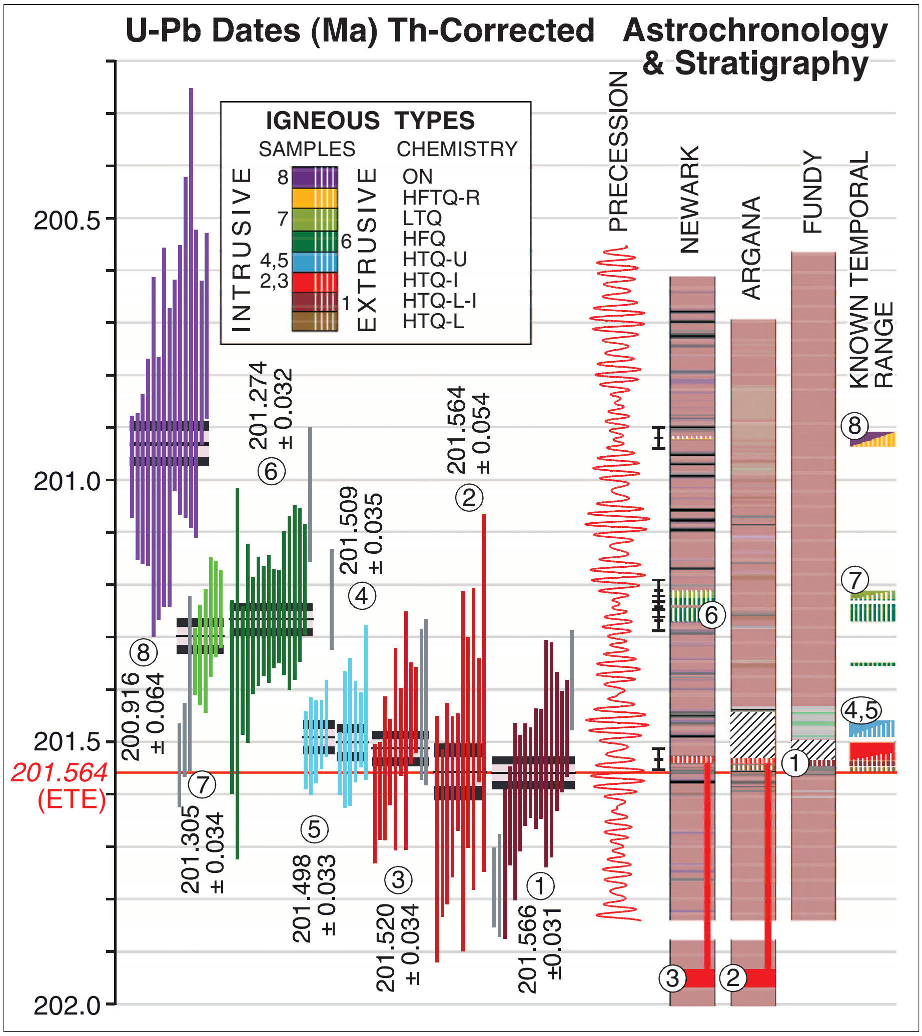

Fig. 2. Zircon U-Pb intercalibration of CAMP volcanism and Early Jurassic Late Triassic astrochronology. Quasiperiodic precessional cyclicity (red) used to generate the ATS (*9*, *28*). Within the stratigraphic sections (right), black- and white-hatched regions mark depositional hiatuses, and error bars next to each basalt mark each unit's timing and uncertainty calculated from the ATS. Colored vertical bars (left) represent the ^{238}U-^{206}Pb Th-corrected dates (*18*) for single-crystal zircon analyses at 2σ, where color indicates basalt chemistry (legend). Legend abbreviations: HTQ, high-titanium quartz normative, includes the lower (L), lower-intermediate (L-I), intermediate (I), and upper (U) units; HFQ, high-iron quartz normative; LTQ, low-titanium quartz normative; HFTQ-R, high–iron-titanium quartz normative or recurrent unit; and ON, olivine normative units. Grayed analyses are excluded from calculated mean dates (*18*). Sample numbers: 1, North Mountain Basalt; 2, Amelal sill; 3, Palisades sill; 4, York Haven intrusive; 5, Rapidan intrusive; 6, Preakness Basalt; 7, Rossville intrusive; 8, Butner intrusive. Reported dates and black horizontal line mark the weighted mean date, and the outer horizontal box marks the 2σ uncertainty. Tabulated data, including a second dated North Mountain Basalt sample, are reported in table S1 (*18*).

Newark section, each horizon dated by U-Pb can be placed within the astrochronologic time scale and assigned an estimated time since the ETE (i.e., the extinction horizon that cannot be directly dated by geochronology) (Fig. 3B). Comparing the U-Pb geochronology and the durations between the ETE and the dated flows implied by the astronomical tuning reveals that the two chronologies agree well given the analytical uncertainties in the U-Pb dates and the ± 20 ky uncertainties assigned to the astrochronology. Combining the two data sets (Fig. 3B), the U-Pb dates anchor the higher-precision astrochronology in absolute time, and a least-squares optimization can be used to simultaneously solve for the absolute date of the ETE as well as those of the dated samples that best fit the relative and absolute timing constraints (table S2) (*18*). This approach yields an estimate of the ETE of 201.564 ± 0.015/0.22 Ma, with a χ^2_{red} (mean square weighted deviation) of 1.3, where the first uncertainty reflects analytical uncertainty only and the second includes uncertainty in the ^{238}U, ^{232}Th, and ^{230}Th decay constants. U-Pb geochronologic data are therefore consistent with our geochemical model and assumed correlations and validates the use of the ATS for high-resolution astrochronology for the CAMP and ETE time interval. This further indicates that orbital signals were faithfully recorded in these lacustrine strata and that solar system dynamics along with the duration of precession cycles 200 Ma can be reliably modeled (*29*).

The Relationship Between the Eruption of CAMP and the End-Triassic Extinction

Integration of geochronologic, geochemical (*11*, *21*–*23*, *25*, *30*), paleontological (*9*, *11*, *31*), and magnetostratigraphic (*25*, *32*, *33*) data for the Newark, Fundy, and Argana basins provide the basis for a high-resolution chronology of the earliest known CAMP eruptions and the extinction event (Fig. 4). In each of these sections, the magnetic polarity chron E23r is observed below the sporomorph turnover that marks the terrestrial ETE. The assumed global synchroneity of both magnetic reversals and mass extinctions at the thousand-year level suggests that a common time duration is shared between the horizons marking the base of the E23r and the ETE. If we assume to first order that the thickness of lacustrine strata between these horizons is a proxy for time, the thickness of sedimentary rocks defines the relative duration between the ETE and the lowermost basalts in each basin (Fig. 4). This relative chronology implies that the base of the North Mountain Basalt of the Fundy basin is older than the base of the Orange Mountain Basalt of the Newark basin, whereas the lowermost basalt within the Argana basin (Tasguint Basalt) is older still than the North Mountain Basalt, placing the Tasguint basalt as the oldest CAMP unit. Time estimates on the sedimentary interval from E23r to the lowermost basalt are provided through integration with the astrochronologic time scale for the Newark basin. Within the Newark basin, the base of E23r to the ETE coincides with one climatic precession cycle (*2*), thus permitting the precession cycle duration to be correlated to the E23r to ETE interval in both the Fundy and Argana basins (Fig. 4). For a 5-million-year duration of the precession parameter, the average climatic precession cycle is 21.1 ± 6.1 ky (2σ), with a range of 10 to 31 ky. For the Late Triassic–Early Jurassic (200 Ma), that would be ~19.8 ± 5.7 ky due to the recession of the Moon (*29*). Using this model, the ETE is about 13.2 ± 3.8 ky older than the Orange Mountain Basalt (range of 12.9 to 13.5 ky, depending on the section). The base of the North Mountain Basalt of the Fundy basin is about 10.0 ± 2.9 ky older than the base of the Orange Mountain Basalt, which is 3.2 ± 0.9 ky younger than the ETE, and the base of the Tasguint Basalt is 13.2 ± 3.8 ky older than the Orange Mountain and 3.2 ± 0.9 ky older than the North Mountain Basalt.

Both the turnover in sporomorph taxa marking the terrestrial ETE and an interval of post-ETE strata is observed below the lowermost basalts in both the Newark and Fundy basins, implying that within these basins CAMP basalts postdate the extinction. The palynological turnover is, however, not observed within the Argana basin, where Triassic sporomorphs are continually observed within sedimentary rocks up to the base of the Tasguint basalt (*11*). The combined evidence of (i) the older age of the Tasguint basalt relative to basalts in the Newark and Fundy basins, (ii) the astrochronologic time constraints on sediment deposition for the E23r-basalt interval, and (iii) the presence of Triassic sporomorphs beneath the Tasguint basalt, all place the extinction horizon at the base of or within the Tasguint basalt, consistent with the model by Deenen and others (*25*) but conflicting with chronology of Marzoli and others (*11*). This chronologic framework permits a causal relationship between CAMP and the ETE to be made at a high level of precision.

Although this temporal link between the eruption of CAMP and ETE strongly imply a causal relationship, how the eruption of CAMP induced a global extinction remains unclear. An emerging model requires the near-instantaneous eruption of large volumes of magma (~8×10^5 km^3) in order to explain (i) the apparent increase of atmospheric pCO_2 values (*12*, *13*, *34*); (ii) the near collapse of coral reefs and absence of carbonate deposition, both thought to be triggered by the decrease in the pH of ocean seawater (*14*, *15*); and (iii) the approximately 5–8.5 per mil negative excursion in organic δ^{13}C values observed in both marine and terrestrial records, suggesting a large input of isotopically light carbon into the atmosphere (*35*–*37*). The subsequent biologic recovery from this extinction is marked within marine sections at the Triassic-Jurassic Boundary (TJB) (*38*), which is defined at its Global Boundary Stratotype

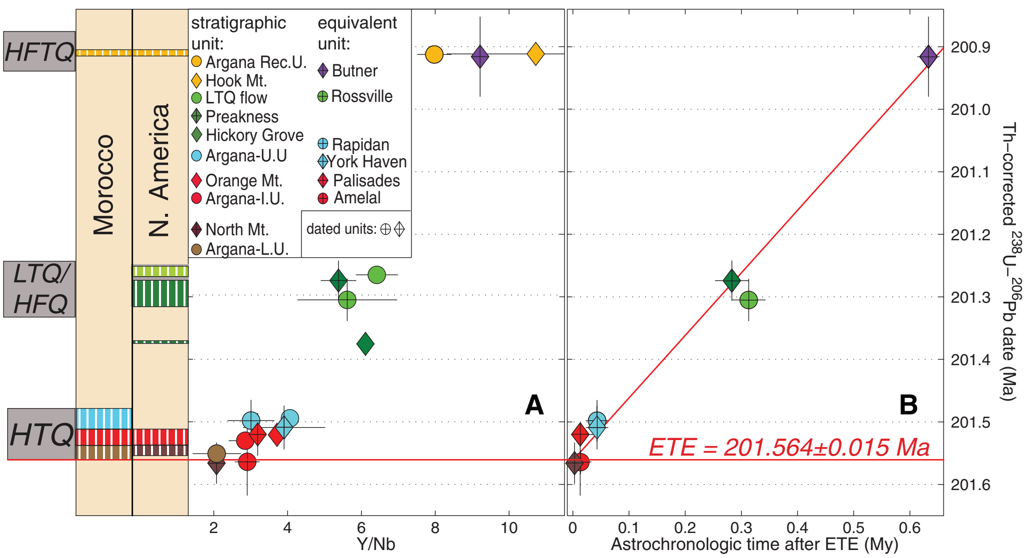

Fig. 3. Geochemical evolution of CAMP magmas and the comparison between astrochronologic and geochronologic time scales. (**A**) Geochemical evolution for CAMP units is observed in relative time (stratigraphic column, far left) and in geochronologic time. Included for completeness is the undated Hickory Grove Basalt in the Culpeper basin of Virginia. (**B**) Using a geochemical correlation between stratigraphically constrained basalts and the dated intrusives (equivalent units), U-Pb dates from all dated CAMP units are correlated to the Newark basin and assigned an elapsed time since the ETE. Within the U-Pb and astrochronologic uncertainties, a least-squares optimization reaffirms the reliability of the astrochronologic time scale and the assumptions associated with the geochemical correlation.

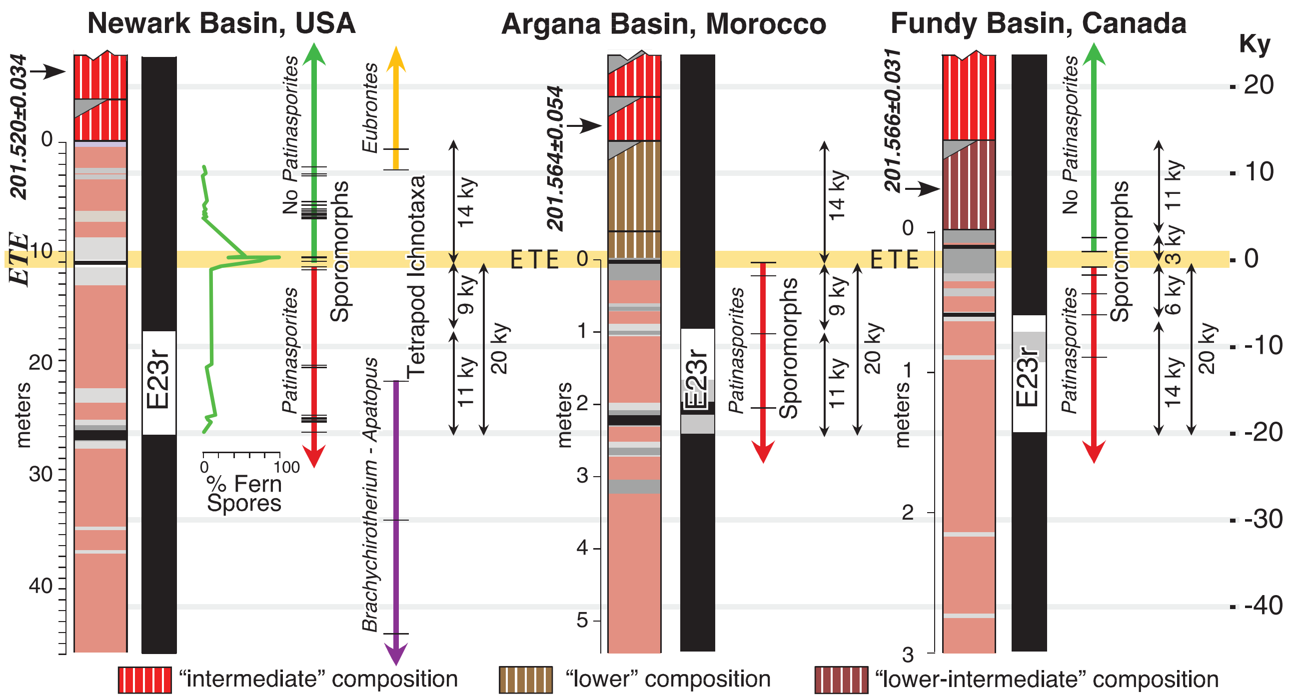

Fig. 4. Integration of geochronologic, magnetostratigraphic, and palynologic data sets for the stratigraphic interval from E23r to the lowermost CAMP basalts in the Newark, Argana, and Fundy basins. Basalt U-Pb dates and magnetic reversal E23r permit correlation between sections. Basalt color correlates to chemistry. Labeled black arrows indicate the astrochronologic time estimates in thousands of years (ky). Palynological data reveal a turnover (green to red arrow transition) in sporomorphs beneath the lower basalt of the Newark and Fundy basin, marking the ETE (yellow horizontal line) at a horizon below the basal CAMP in these basins.

Section and Point (GSSP) as the first appearance of the ammonite *Psiloceras spelae* (*39*). At the GSSP and throughout northern Europe (*35*), correlation to the Newark Basin and the ATS (*36*) places the TJB at ~100 ± 40 ky after the ETE (where the large uncertainty derives from problems correlating the marine and terrestrial astrochronologic cycles) and after the eruption of the older, upper high-titanium quartz normative (HTQ-U) basalts. This timeline implies that the biologic recovery associated with the TJB was under way even as subsequent CAMP eruptions and associated pulsed increases in atmospheric CO_2 (*13*) were occurring ~60 ky (HTQ-U), ~270 ky [high-iron quartz normative (HFQ/low-titanium quartz normative (LTQ)], and ~620 ky [high–iron-titanium quartz normative (HFTQ-R) after the extinction event (Fig. 3). Because our geochronologic data resolve four discrete CAMP pulses, we propose that it is the first pulse of the “lower” and “intermediate” HTQ chemical groups (Fig. 4) that erupted coincident with and immediately after the ETE that caused the global extinction.

References and Notes

1. V. E. Courtillot, P. R. Renne, *C. R. Geosci.* **335**, 113 (2003).
2. P. E. Olsen *et al.*, in *Catastrophic Events and Mass Extinctions: Impacts and Beyond,* C. Koeberl, K. G. MacLeod, Eds. (Geological Society of America Special Paper, Boulder, CO, 2002), vol. 356, pp. 505–522.
3. M. J. Benton, *Science* **268**, 52 (1995).
4. N. Morton, *Int Subcomm Jurassic Stratigr Newslett* **35**, 74 (2008).
5. A. Marzoli *et al.*, *Science* **284**, 616 (1999).
6. B. Schoene, J. Guex, A. Bartolini, U. Schaltegger, T. J. Blackburn, *Geology* **38**, 387 (2010).
7. G. McHone, *Volatile Emissions from Central Atlantic Magmatic Province Basalts: Mass Assumptions and Environmental Consequences* (American Geophysical Union, Washington, DC, 2003), vol. 136, p. 14.
8. P. E. Olsen, D. V. Kent, M. Et-Touhami, J. H. Puffer, in *The Central Atlantic Magmatic Province: Insights from Fragments of Pangea,* W. E. Hames, G. McHone, P. R. Renne, C. Ruppel, Eds. (Geophysical Monograph Series, 2003), vol. 136, pp. 7–32.
9. J. H. Whiteside, P. E. Olsen, D. V. Kent, S. J. Fowell, M. Et-Touhami, *Palaeogeogr. Palaeoclimatol. Palaeoecol.* **244**, 345 (2007).
10. F. Jourdan *et al.*, *Lithos* **110**, 167 (2009).
11. A. Marzoli *et al.*, *Geology* **32**, 973 (2004).
12. J. C. McElwain, D. J. Beerling, F. I. Woodward, *Science* **285**, 1386 (1999).
13. M. F. Schaller, J. D. Wright, D. V. Kent, *Science* **331**, 1404 (2011).
14. B. Hönisch *et al.*, *Science* **335**, 1058 (2012).
15. S. E. Greene, D. J. Bottjer, F. A. Corsetti, W. M. Berelson, J.-P. Zonneveld, *Geology* **40**, 1043 (2012).
16. A. Robock, *Rev. Geophys.* **38**, 191 (2000).
17. D. Gottfried, L. P. Greenland, E. Y. Campbell, *Geochim. Cosmochim. Acta* **32**, 925 (1968).
18. Materials and methods are available as supplementary materials on *Science* Online.
19. J. H. Puffer, K. A. Block, J. C. Steiner, *J. Geol.* **117**, 139 (2009).
20. H. El Hachimi, thesis, Cadi Ayyad University, Marrakesh, Morocco (2012).
21. D. Gottfried, A. Froelich, J. N. Grossman, “Geochemical data for Jurassic diabase associated with early Mesozoic basins in the eastern United States; Gettysburg Basin and vicinity, Pennsylvania and Maryland,” Open-File Report 91-322-E (USGS, Washington, DC, 1991); http://pubs.er.usgs.gov/publication/ofr91322E.
22. D. Gottfried, A. Froelich, J. N. Grossman, “Geochemical data for Jurassic diabase associated with early Mesozoic basins in the eastern United States; Culpeper Basin and vicinity, Virginia and Maryland,” Open-File Report 91-322-F (USGS, Washington, DC, 1991); http://pubs.er.usgs.gov/publication/ofr91322F.
23. D. Gottfried, A. Froelich, J. N. Grossman, “Geochemical data for Jurassic diabase associated with early Mesozoic basins in the eastern United States; western Newark Basin, Pennsylvania and New Jersey,” Open-File Report 91-322-C (USGS, Washington, DC, 1991); http://pubs.er.usgs.gov/publication/ofr91322C.
24. R. P. Tollo, D. Gottfried, *Spec. Pap. Geol. Soc. Am.* **268**, 233 (1992).
25. M. H. L. Deenen *et al.*, *Earth Planet. Sci. Lett.* **291**, 113 (2010).
26. L. A. Hinnov, J. G. Ogg, *Stratigraphy* **4**, 239 (2007).
27. F. B. VanHouten, *Am. J. Sci.* **260**, 561 (1962).
28. P. E. Olsen, D. V. Kent, *Palaeogeogr. Palaeoclimatol. Palaeoecol.* **122**, 1 (1996).
29. A. Berger, M. Loutre, J. Laskar, *Science* **255**, 560 (1992).
30. J. N. Grossman, D. Gottfried, A. J. Froelich, “Geochemical data for Jurassic diabase associated with early Mesozoic Basins in the eastern United States,” Open-File Report 91-322-J (USGS, Washington, DC, 1991); http://pubs.er.usgs.gov/publication/ofr91322J.
31. S. Cirilli *et al.*, *Earth Planet. Sci. Lett.* **286**, 514 (2009).
32. D. V. Kent, P. E. Olsen, *J. Geophys. Res.* **104** (B6), 12831 (1999).
33. M. H. L. Deenen, W. Krijgsman, M. Ruhl, J.-C. Mareschal, *Can. J. Earth Sci.* **48**, 1282 (2011).
34. M. R. Rampino, K. Caldeira, *Science* **334**, 594, author reply 594 (2011).
35. S. P. Hesselbo, S. A. Robinson, F. Surlyk, S. Piasecki, *Geology* **30**, 251 (2002).
36. J. H. Whiteside, P. E. Olsen, T. Eglinton, M. E. Brookfield, R. N. Sambrotto, *Proc. Natl. Acad. Sci. U.S.A.* **107**, 6721 (2010).
37. M. Ruhl, N. R. Bonis, G.-J. Reichart, J. S. Sinninghe Damsté, W. M. Kürschner, *Science* **333**, 430 (2011).

38. A. Bartolini *et al.*, *Geochem. Geophys. Geosyst.* **13**, Q01007 (2012).
39. A. von Hillebrandt, L. Krystyn, *Geologie und Palontologie* **253**, 163 (2009).
40. D. V. Kent, L. Tauxe, *Science* **307**, 240 (2005).

Acknowledgments: We express our gratitude to S. Burgess, N. Youbi, B. Schoene, J. Ramezani, D. Condon, and two anonymous reviewers. We acknowledge that this work owes much to the collective effort of the EARTHTIME community. We also thank Vulcan Materials and Carolina Sunrock LLC for quarry access, G. Fisher of the Alcatel-Lucent EH&S-Americas for Preakness Basalt cores, B. Smith for the Rossville and York Haven diabase samples, and J. Smoot and N. Ratcliff for access to cores and thin sections. We acknowledge support from the U.S. National Science Foundation (grants EAR-0446880 and EAR-0931839 to S.A.B., EAR 0753496 to P.E.O. and D.V.K., and EAR 0345664 to E.T.R.). P.E.O. received support from the Bahamas Petroleum Company. Data presented in this paper are fully documented in the supplementary materials. U-Pb zircon data are deposited at the Geochron database (www.geochron.org) with SESAR IGSNs SAB000002-SAB00000A, available at www.geochron.org/dataset/html/5QlSoX9SCtJbNfOZbNeXtuwSK.

Supplementary Materials
www.sciencemag.org/cgi/content/full/science.1234204/DC1
Materials and Methods
Supplementary Text
Figs. S1 to S5
Tables S1 to S3
References (*41–92*)

18 December 2012; accepted 28 February 2013
Published online 21 March 2013;
10.1126/science.1234204

Annually Resolved Ice Core Records of Tropical Climate Variability over the Past ~1800 Years

L. G. Thompson,[1,2]* E. Mosley-Thompson,[1,3] M. E. Davis,[1] V. S. Zagorodnov,[1] I. M. Howat,[1,2] V. N. Mikhalenko,[4] P.-N. Lin[1]

Ice cores from low latitudes can provide a wealth of unique information about past climate in the tropics, but they are difficult to recover and few exist. Here, we report annually resolved ice core records from the Quelccaya ice cap (5670 meters above sea level) in Peru that extend back ~1800 years and provide a high-resolution record of climate variability there. Oxygen isotopic ratios ($\delta^{18}O$) are linked to sea surface temperatures in the tropical eastern Pacific, whereas concentrations of ammonium and nitrate document the dominant role played by the migration of the Intertropical Convergence Zone in the region of the tropical Andes. Quelccaya continues to retreat and thin. Radiocarbon dates on wetland plants exposed along its retreating margins indicate that it has not been smaller for at least six millennia.

Ice cores from high-altitude tropical glaciers offer long-term perspectives on the variability of precipitation, temperature, aridity, and atmospheric and sea surface conditions at low latitudes. Most meteorological and climatic disturbances affecting Earth's surface and lower atmosphere originate in or are amplified by ocean-atmosphere interactions in tropical latitudes. As Earth's "heat engine," the warmest atmospheric and sea surface temperatures (SSTs) occur there. This energy drives intense convective precipitation and is crucial for the evolution of phenomena such as El Niño–Southern Oscillation (ENSO), the monsoonal systems of Asia and Africa, and, on intraannual time scales, hurricanes and other tropical disturbances that distribute equatorial heat energy poleward. ENSO dominates tropical climate variability. It is linked to the position of the Intertropical Convergence Zone (ITCZ), and its associated teleconnections affect the strength and direction of air masses and storm tracks, variations in convective activity that control flooding and drought, and modulation of tropical storm intensities. There are few high mountain glaciers in these regions and even fewer that preserve detailed histories of this variability. Unfortunately, most are now rapidly shrinking, and unique records are being lost. The potential impacts on water resources have social and economic consequences that underpin the imperative to understand the drivers and responses of past and present tropical climate variability.

The first ice cores drilled from the Quelccaya ice cap (QIC) [13°56′S, 70°50′W, 5670 m above sea level (masl)], in 1983 (*1–3*), could not be returned frozen to the laboratory and instead were cut into samples that were melted and bottled in the field. In 2003, two additional cores were drilled to bedrock on the QIC (Fig. 1). The Summit Dome (5670 masl) core (QSD, 168.68 m) and the North Dome (5600 masl) core (QND, 128.57 m) were returned frozen and are stored at –30°C at Ohio State University's Byrd Polar Research Center. Minimal postdepositional reworking of the snow surface, even during the wet season, results in the distinct annual layers (fig. S1A) used to reconstruct an ~1800-year climate history. Details about the construction of the time scale, extracting annually resolved information, and reconstructing the net annual accumulation are provided in the supplementary text. The oxygen isotopic ratio ($\delta^{18}O$) records for the 2003 QSD and QND cores, separated by 1.92 km, are highly correlated ($r = 0.898$, $P < 0.0001$ for decadal averages; table S1). In light of their similarity,

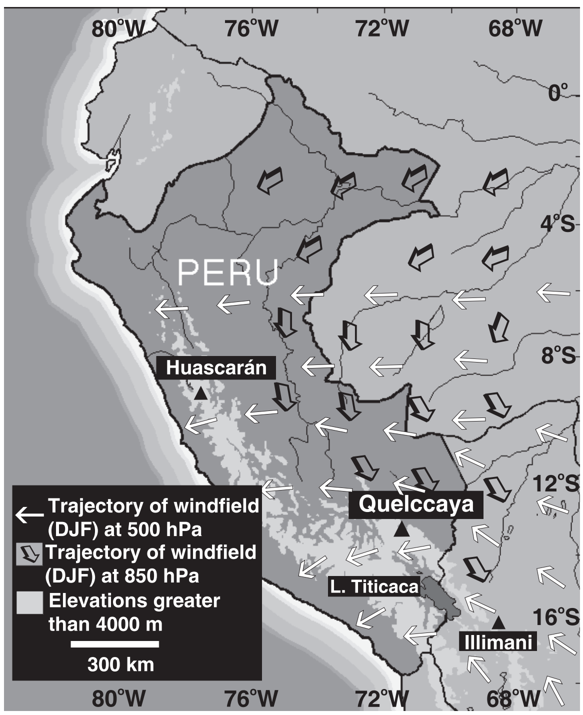

Fig. 1. Location of the QIC, Peru, and other ice fields and features discussed in the text. Also included are the upper (500 hPa) and lower (850 hPa) level atmospheric circulation in the austral summer [December-January-February (DJF)] (*38*).

[1]Byrd Polar Research Center, The Ohio State University, Columbus, OH 43210, USA. [2]School of Earth Sciences, The Ohio State University, Columbus, OH 43210, USA. [3]Department of Geography, The Ohio State University, Columbus, OH 43210, USA. [4]Institute of Geography, Russian Academy of Sciences, Moscow, Russia.

*Corresponding author. E-mail: thompson.3@osu.edu